

SCIENTIFIC REPORTS



OPEN

Robotic lower limb prosthesis design through simultaneous computer optimizations of human and prosthesis costs

Received: 15 September 2015

Accepted: 18 December 2015

Published: 09 February 2016

Matthew L. Handford & Manoj Srinivasan

Robotic lower limb prostheses can improve the quality of life for amputees. Development of such devices, currently dominated by long prototyping periods, could be sped up by predictive simulations. In contrast to some amputee simulations which track experimentally determined non-amputee walking kinematics, here, we explicitly model the human-prosthesis interaction to produce a prediction of the user's walking kinematics. We obtain simulations of an amputee using an ankle-foot prosthesis by simultaneously optimizing human movements and prosthesis actuation, minimizing a weighted sum of human metabolic and prosthesis costs. The resulting Pareto optimal solutions predict that increasing prosthesis energy cost, decreasing prosthesis mass, and allowing asymmetric gaits all decrease human metabolic rate for a given speed and alter human kinematics. The metabolic rates increase monotonically with speed. Remarkably, by performing an analogous optimization for a non-amputee human, we predict that an amputee walking with an appropriately optimized robotic prosthesis can have a lower metabolic cost – even lower than assuming that the non-amputee's ankle torques are cost-free.

People with trans-tibial (below knee) amputation commonly use passive prostheses providing some stiffness and damping (e.g., SACH-foot, Flex-foot¹). However, passive prosthesis users experience reduced mobility^{2,3} and increased metabolic cost^{4,5} compared to non-amputees. This reduced performance is partially due to reduced foot control and an inability to produce net positive work with the prosthesis. Robotic ankle-foot prostheses could address these issues^{6,7}. Although many robotic prostheses exist, designing and testing new prostheses takes considerable time: computational simulations could shorten this process. Many previous simulation studies^{8,9} used human-prosthesis models that tracked non-amputee walking kinematics, thus ignoring human adaptation to the prosthesis¹⁰. Here, rather than assume the amputee's gait, we seek to predict it. Similarly, rather than assume a specific prosthesis actuation strategy, we design prosthesis torque profiles through energy optimization.

Numerous studies suggest that humans move in an approximately energy optimal manner^{11,12}, even with amputation¹³ or using unpracticed motions¹⁴. Here, we use large-scale numerical optimization to compute the energy-optimal walking motions and prosthesis actuations of a human wearing a unilateral robotic prosthesis. We compute optimal trade-offs between human metabolic and prosthesis torque costs. We show how increasing prosthesis mass, using passive prostheses, or forcing left-right symmetry increase human costs for a given walking speed and how increasing speed increases cost. Finally, we predict that optimal prosthesis actuation can reduce the amputee metabolic cost much below normal human metabolic cost.

Methods

Human-prosthesis model. We consider a sagittal plane model of a unilateral amputee using an ankle-foot prosthesis (Fig. 1A) with empirically-based properties^{15,16}. The human component has six rigid-body segments: one head-arms-torso segment, one segment for each thigh, one segment for each shank, and one segment for the biological foot. There are thirteen uni- or bi-articular muscles with constant moment-arms and Hill-type force-velocity relationships: eight muscles on the biological (non-prosthesis) side and five on the prosthesis side. The prosthesis foot is a single rigid-body segment, actuated by an idealized torque motor with no internal

Mechanical and Aerospace Engineering, The Ohio State University, Columbus, USA. Correspondence and requests for materials should be addressed to M.L.H. (email: handford.4@osu.edu) or M.S. (email: srinivasan.88@osu.edu)

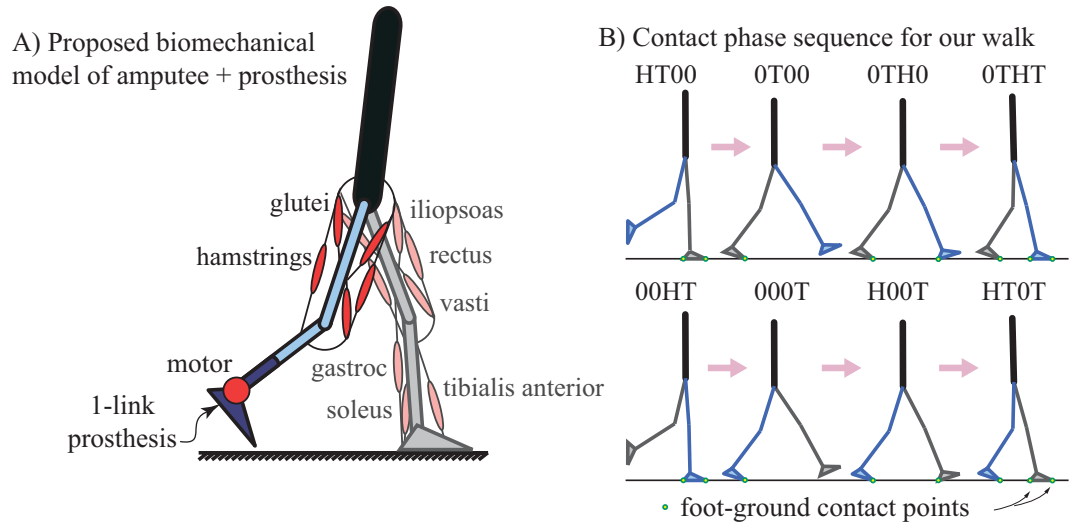


Figure 1. (A) A sagittal-plane rigid-body model, with six human body segments and one prosthesis segment, connected via revolute joints. The leg without amputation uses eight muscles (iliopsoas, gluteus, hamstring, rectus femoris, vastus lateralis, gastrocnemius, soleus, and tibialis anterior); the leg with amputation uses identical muscles but removing and replacing all muscles crossing the ankle with a single prosthesis torque motor at the ankle. (B) Contact phase sequence for a natural walking motion. The four letter code refers to the points contacting the ground; heel and toe of the biological and prosthetic foot with 0 signifying no contact.

dynamics. The prosthetic foot mass and inertia properties are identical to the human foot unless otherwise stated. See Supplementary Information for parameter values. We present all parameters and results in non-dimensional form, normalized by combinations of body mass M_{body} , leg length l_{leg} , and gravitational acceleration g .

The feet can contact the ground at their heel and toe. We assume a normal walking motion with a prescribed sequence of eight ‘contact phases’ (Fig. 1B), each denoted by a four-letter code specifying which heels (H) and toes (T) are in contact or not (0): the first two letters refer to the biological foot’s contact points and the last two letters refer to the prosthesis’. e.g., HT0T has biological heel and toe and prosthesis toe in contact. Contact kinematic constraints are imposed using a differential-algebraic formalism, as opposed to modeling contact with springs and dampers^{16–18}. By assuming that any point in contact with the ground has a zero velocity, this method of imposing contact constraints removes high frequency and fast time-scale dynamics that can arise due to springs and dampers. Given muscle forces and prosthesis torque as functions of time and initial conditions for body state, we can integrate the equations of motion for each contact phase to simulate the motion of the human-prosthesis system. We model transitions between contact phases as continuous when contact is broken and as perfectly-inelastic collisions, with velocity changing instantaneously when contact is made.

Energy cost functions. We seek a periodic walking motion that minimizes \dot{C} , a weighted sum of the human metabolic cost C_{met} and the prosthesis cost C_{pros} over a stride as follows:

$$\dot{C} = (\lambda C_{\text{met}} + (1 - \lambda) C_{\text{pros}}) / T_{\text{stride}} \quad (1)$$

where T_{stride} is the stride time and $0 \leq \lambda \leq 1$ is a fixed weighting factor: $\lambda = 1$ makes \dot{C} identical to human cost and $\lambda = 0$ gives the prosthesis cost. Optimizing with multiple λ values allows us to determine the trade-offs between human metabolic cost and prosthesis cost by changing the relative importance of the two costs in the optimization.

Our human metabolic cost function is adapted from Alexander and Minetti^{11,19}:

$$C_{\text{met}} = \int_0^{T_{\text{stride}}} \left[\sum_i [\psi(a_i) + a_i \phi(\bar{v}_i)] F_{\text{iso},i} v_{\text{max},i} \right] dt, \quad (2)$$

an integral over the whole stride period and a sum over all muscles, depending on activation a_i , shortening velocity v_i , maximum shortening velocity $v_{\text{max},i}$ and maximum isometric force $F_{\text{iso},i}$; $\psi(a_i)$ is an activation-related cost and $\phi(\bar{v}_i)$ is a function¹¹ describing the metabolic dependence on normalized muscle shortening velocity

$$\bar{v}_i = v_i / v_{\text{max},i} \quad (3)$$

(see Supplementary Information, Figure S2). The prosthesis cost is modeled as

$$C_{\text{pros}} = \int_0^{T_{\text{stride}}} [(\tau/r)^2 + \varepsilon(\dot{\tau}/r)^2] dt, \quad (4)$$

where τ is the motor torque, $\dot{\tau}$ is the torque-rate, and r is a scaling constant (equal to typical muscle moment arm); the torque-squared term is a model of motor electrical losses²⁰ and the torque-rate-squared term with a small pre-multiplier ($\varepsilon = 0.01$) is used to model torque production limitations by penalizing rapid activation and deactivation^{11,21}.

Other metabolic cost models. While all the results in the main manuscript are based on the above cost functions for the human and the prosthesis, we also considered two other simple cost functions that have previously been used in biomechanics to model “effort” or metabolic cost: (1) cost rate for each muscle proportional to muscle-force squared^{16,22}, and (2) energy cost for each muscle proportional to a weighted sum of positive and negative work, scaled by the efficiencies of positive and negative work^{11,23}. We did not use other more complex models based on muscle heat generation^{18,24}, as they are often non-smooth; we will consider such functions in future work.

Optimization structure and constraints. We seek an optimal walking gait with the periodic contact phase sequence in Fig. 1B, parameterized using a “multiple-shooting method”. We constrained speed at $v = 1.3$ m/s or non-dimensional speed $\bar{v} = v/\sqrt{g\ell_{\text{leg}}} = 0.42$, except for one set of calculations that varied speed systematically. The eight contact phases, $N_{\text{phases}} = 8$, each with unknown time duration, are divided into $N_{\text{seg}} = 6$ time-segments, each with $N_{\text{unknowns}} = 32$ unknowns (initial conditions for all body segment positions and velocities and unknown muscle forces and prosthesis motor torque, assumed piecewise linear), producing 1544 unknowns through:

$$N_{\text{phases}} + N_{\text{phases}}N_{\text{unknowns}}N_{\text{seg}} = N_{\text{total-unknowns}} \quad (5)$$

to be determined by optimization. We constrain positions, velocities, forces and torques to be continuous across different time segments. For collisional transitions, the results of the collision equations (applied to the end of the contact phase) are equal to the initial conditions for the next contact phase. Further nonlinear constraints include ground clearance for swing legs, ground contact for stance legs, muscle force-velocity dependence, and range of motion bounds. We solve the constrained optimization problem using sparse nonlinear programming (SNOPT¹¹), with equality constraint satisfaction of 10^{-7} . Since it is possible for the optimization to converge to non-global local minima, we only consider solutions which can be discovered from multiple initial seeds.

Results

Optimizing just the human cost (mostly). We minimized the composite cost \hat{C} strongly weighted towards human cost ($\lambda = 0.95$), to obtain optima when prosthesis cost is mostly neglected. Figure 2A,B and the walking animations (Supplementary Video V1) show the corresponding optimal motion is asymmetric.

Setting $\lambda = 1$ caused convergence issues in the numerical optimization; presumably because this limit $\lambda = 1$ implies a truly “zero cost prosthesis,” the optimization tended to explore large and erratic prosthesis motor torques and torque rates, resulting in the numerical difficulties.

Comparison with non-amputee gait. We minimized the same human metabolic cost for a non-amputee (able-bodied) human with symmetric legs and musculature, giving a symmetric optimal gait (Fig. 2A,B). Metabolic cost for the amputee with a prosthesis is lower than that for the non-amputee (Fig. 3A). The muscles crossing a single ankle contribute 41% of the optimized non-amputee metabolic cost. Thus, if ideal motor torques replaced all muscles crossing one ankle while maintaining identical kinematics, the human cost could be reduced by 41% by this “muscle replacement strategy”. Remarkably, for $\lambda = 0.95$, the human cost with a unilateral prosthesis is 73% lower than the non-amputee cost. This greater cost reduction arises from allowing amputee kinematics to be different from non-amputee kinematics, thus allowing the prosthesis ankle motor to perform much more work than the replaced ankle muscles. This is remarkable because while the replaced ankle muscles provide torques at both ankle and knee (some muscles are biarticular), our prosthesis produces torques only at the ankle. Thus, extrapolating this trend, we speculate that if we made the prosthesis provide torques at the knee (simulating a supplementary knee exoskeleton) as well as at the ankle, perhaps the optimal cost reduction might be even greater.

Optimal trade-offs between human and prosthesis cost. By optimizing with different λ 's between 0.1 and 0.95, we obtain the optimal cost trade-off between human and prosthesis costs (Fig. 3A). This trade-off curve, often called a “Pareto curve”²⁵, shows that increasing prosthesis cost decreases human cost. Here, even though obtained by minimizing a weighted sum of human and prosthesis cost, the Pareto curve (if ‘convex’) also has the following interpretation: this curve gives the lowest human cost for a given prosthesis cost and vice versa. Any other walking strategy will have either a higher human cost or a higher prosthesis cost compared to every point on this Pareto curve. Figure 3B shows that the the optimal prosthesis actuation has most of prosthesis action at the end of stance phase, providing large push-off power; the human cost is reduced through an increase in prosthesis push-off torque and impulse. While the trade-off in Fig. 3A is specific to the assumed human and prosthesis costs, we find that almost identical trade-off curves arise when substantially different cost functions are used (Figure S3, Supplementary Information).

Symmetry is expensive. Every Pareto-optimal gait we found was asymmetric irrespective of λ . However, walking symmetry is said to have physiological and psychological benefits to prosthesis users²⁶, so we repeated the optimizations while requiring approximate left-right symmetric kinematics. Symmetry was enforced as a constraint requiring the left leg joint angles and angular rates during one step be nearly equal to (within 0.05 rad or 0.05 rads⁻¹ of) the right leg joint angles and angular rates one step later. The resulting symmetric optimal gaits

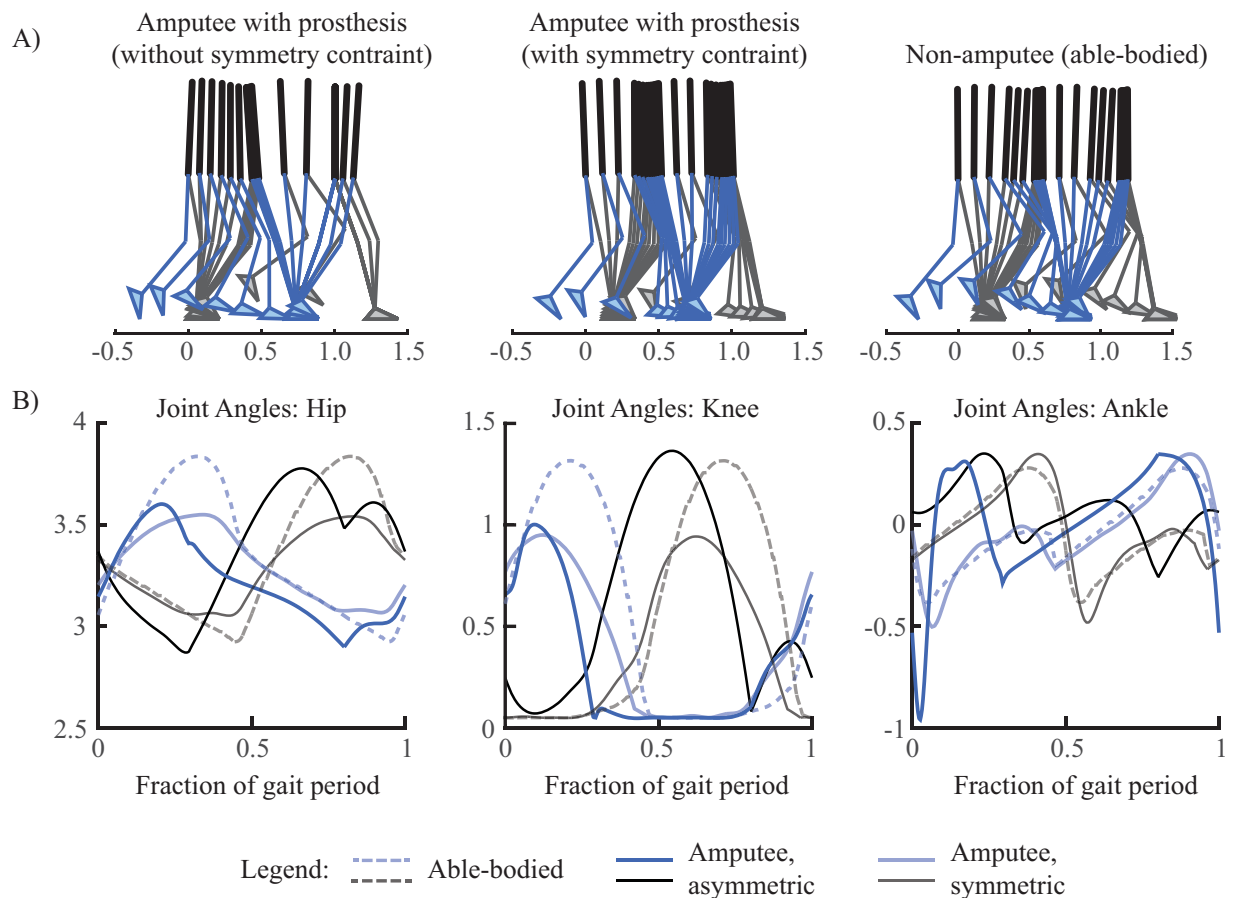


Figure 2. (A) Optimal gait kinematics for amputee walking (with and without symmetry constraint) with $\lambda = 0.95$ and non-amputee walking. For the amputee, the blue leg represents the prosthesis and the black leg represents the biological one. (B) Optimal joint angles for all three conditions over one gait cycle with periods of 2.876 (asymmetric), 2.412 (symmetric), and 2.857 (non-amputee). See Supplementary Video V1 for a video animation of these optimized walking motions.

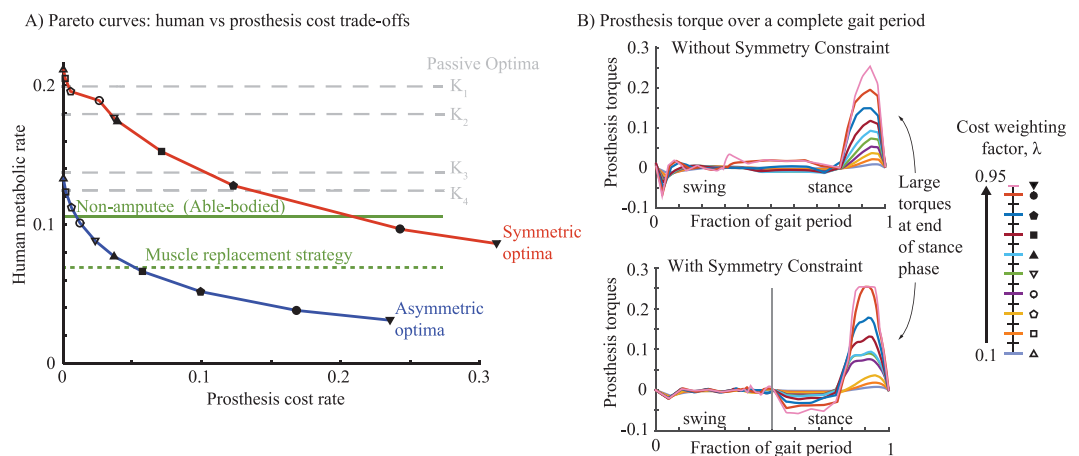


Figure 3. (A) Optimal trade-offs (Pareto curves) between human and prosthesis costs: without symmetry constraint (blue line) and with symmetry (red line). Different markers (legend) denote results from different λ 's (0.1–0.95). Optima from passive prostheses are shown for four non-dimensional stiffnesses (gray dashed line, $K_1 = 0.1$, $K_2 = 0.5$, $K_3 = 1.0$, $K_4 = 1.5$), as are non-amputee optimum (green line) and the non-amputee optimum (green dotted line) with muscle replacement strategy (cost-free ankle muscle costs). See Figure S3 (Supplementary Information) for analogous Pareto trade-off curves for two other metabolic cost models. (B) Prosthesis torque over one stride with gait symmetry unconstrained and constrained. Each line represents an optimization with different λ (0.1–0.95). The labels 'swing' and 'stance' are left without a clear demarcation of when these phases occur, because they are different durations for the different optimal gaits when asymmetry is allowed; with symmetry, each of these phases is 50% of the gait period.

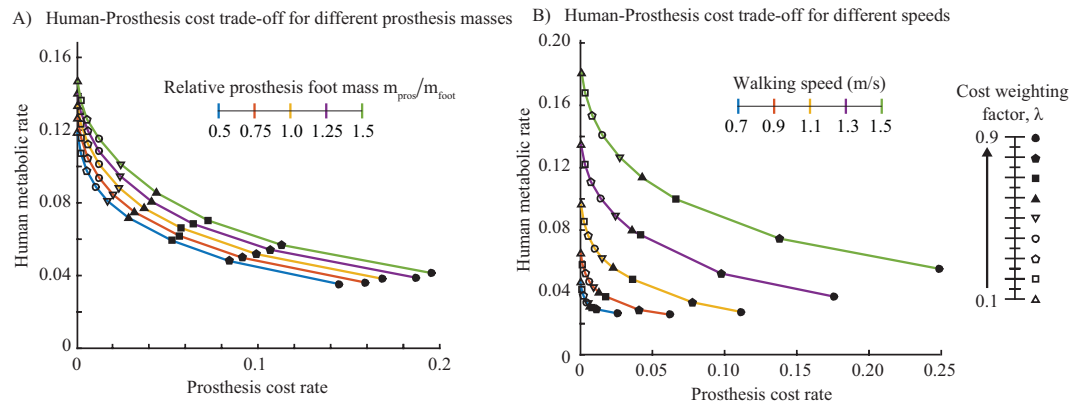


Figure 4. (A) Pareto curves between human and prosthesis cost for five different prosthetic foot masses. Lower prosthetic foot mass is better. (B) Pareto curves with five different walking speeds. Lower speeds have lower costs.

had much higher human and prosthesis costs (Fig. 3A) for each λ , a longer push-off phase, and different timing for dorsiflexion torques during swing phase (Fig. 3B). When we compared the cost of the optimal symmetric gait at $\lambda = 0.95$ to the non-amputee condition, we found only a 27% reduction in the metabolic cost. This reduction in cost is smaller than the 41% metabolic cost reduction achieved by the replacement strategy. The optimal symmetric gait with the prosthesis is worse than the simple replacement strategy, even though the replacement strategy would also result in a symmetric gait; while we do not know the reason for these relative costs, presumably the optimal symmetric gait with the prosthesis has a higher cost because it is unable to replace the knee torques with the prosthesis (no Gastrocnemius), requiring other muscles to compensate.

Lighter feet are less expensive. We performed optimizations with prosthetic foot masses from 50%–150% that of the intact foot, scaling the prosthesis moments of inertia similarly. Figure 4A shows that by fixing either the human or the prosthesis cost, we can reduce the other by reducing prosthesis mass. Further, we see that cost reductions from reducing foot mass are much smaller than those obtained by increasing the prosthesis cost. Both human and prosthesis costs seem well-approximated by a linear dependence on the prosthesis mass for each λ (Figure S4, Supplementary Information), but the coefficients of the linear fit depends on λ .

Greater human cost reduction at higher speeds. We performed optimizations with five different walking speeds between 0.7 and 1.5 m/s, computing the Pareto curves with $\lambda = 0.1$ –0.9. As is true for non-amputee walking, the human metabolic rate increases with increasing speed (Fig. 4B). In particular, the whole Pareto curve for a lower speed is below and to the left of that for a higher speed, implying that for a given Prosthesis cost rate, a lower speed implies a lower human metabolic rate and vice versa. Further, we see that for lower speeds, we predict lower percentage and absolute reduction to the human metabolic rate while using an optimal active prosthesis with most human benefit (here $\lambda = 0.9$).

Passive prosthesis. We performed optimizations constraining the prosthesis to be a linear torsional spring and damper, simulating a passive prosthesis. We considered four stiffnesses: 0.10, 0.50, 1.00 and 1.50 non-dimensional stiffness normalized by bodyweight, chosen to roughly capture the torque-angle relationship of optima derived earlier. Damping was chosen to make the foot over-damped during swing; we used $B_{\text{pro}} = 1.73 \cdot 2\sqrt{I_{\text{pro}}K_{\text{pro}}}$, where B_{pro} is the damping, I_{pro} is the prosthesis moment of inertia, K_{pro} is the torsional stiffness, and $2\sqrt{I_{\text{pro}}K_{\text{pro}}}$ is the critical damping value for a second order linear system. While the metabolic cost decreases as the stiffness increased, all of these passive devices produced asymmetric and metabolically expensive human gaits (Fig. 3A). Human cost with the passive device is comparable to active prosthesis with a symmetry constraint, except for high λ 's. Thus, the symmetry constraint is so detrimental as to make active robotic prostheses have little to no energetic benefit over passive devices.

Discussion

We have obtained the optimal tradeoffs between human and prosthesis costs for a robotic unilateral prosthesis, and have suggested that we can reduce amputee metabolic cost by increasing prosthesis effort, allowing asymmetry and decreasing prosthesis mass. These relationships can inform prosthesis design, e.g., by selecting a desired metabolic cost, we could predict the prosthesis cost at various prosthesis masses; the prosthesis torques and costs along with information on number of steps walked daily will allow us to pick motor and battery specifications for the prosthesis. We have created a design tool that translates a specification of the level of assistance to be provided by the prosthesis (namely, λ) into appropriate prosthesis torque profiles.

We have not compared predicted human kinematics and performance with experiment. Such comparison requires implementing our optimal actuation in a prosthesis; a simpler comparison might involve using a passive prosthesis in experiment and comparing with the corresponding model-derived optimal human kinematics. Highly accurate prediction of even non-amputee walking kinematics in a wide variety of novel situations remains

an open problem; recent attempts have fallen short of quantitatively predicting the correct kinematics, kinetics, and/or metabolic costs^{16–18}, even though having qualitatively similar kinematics, analogous to our non-amputee optimization here. Improved predictions of human walking with a prosthesis may require more complex human body models, more accurate metabolic cost models, and inclusion of other objectives such as lowered interaction forces between human and prosthesis.

Our optimization predicts asymmetric gaits for both robotic and passive prostheses but the mechanism that causes the asymmetry is likely different in these two settings. When using a passive prosthesis, the gait becomes asymmetric since the prosthesis cannot add positive work to the system and the human is compensating with the intact limb. However, for robotic prostheses, our model suggests asymmetric gaits are energy optimal with symmetric gaits costing vastly more. In these asymmetric optimal gaits, the leg with the prosthesis spends more time on the ground (higher duty factor, Figure S5, Supplementary Information) compared to the biological leg, allowing the robotic prosthesis to provide greater assistance; we predict that optimal prosthesis actuation could reduce the human cost, possibly much below non-amputee levels (by over 70%). This energy reduction prediction is considerably higher than observed in experimental studies, which have at best reduced the users' metabolic costs to about equal to non-amputee metabolic cost²⁷ (about 14% reduction compared to the subjects' passive prostheses).

This discrepancy in energy costs is likely because our predictions are based on simultaneous optimization of human and prosthesis control and therefore a best case scenario, whereas the controllers in current robotic prostheses are not generally optimized to the person and the person may also not have had enough time to adapt to the prosthesis. Our optimal prosthesis actuation as a function of time has a large torque impulse near the end of the stance phase; it may be that current robotic prostheses, with their simpler ankle-state-based feedback controllers, are unable to allow the prosthesis to produce a large torque impulse right at the end. Most current prosthesis also have a lower peak torque than allowed in our simulations, as our peak torque was based on a recent physical prosthesis emulator²⁸, reported as having the higher torque output among current prostheses. Further, whereas our prosthesis actuation is specific to walking at a particular speed on level ground, the feedback controllers in current robotic prostheses may have been the result of compromises made for use at different walking speeds, slopes, etc. Producing large energy reductions in experiment may require a prosthesis capable of optimizing its torque output to the person and the environment (perhaps over a training period). Other issues that compound the discrepancy in costs between current prostheses and our predictions include secondary goals sought by the user (e.g. gait symmetry, pain reduction, lateral-stability, etc.), or other un-modeled effects.

Alternatively, it may be that the large energy reduction we predict is due to our specific metabolic cost model. Experimental studies in non-amputees suggest that each ankle contributes about 13% of the metabolic cost of walking²⁹ while our metabolic cost model predicts a total of 41%. Repeating the non-amputee calculation with a work-based metabolic cost, we found that only about 18% of the total work cost is due to one ankle – this is the reduction predicted by a muscle replacement strategy for this work-based cost (Figure S3 and Table S5, Supplementary Information). For this work-based cost, the robotic prosthesis (with $\lambda = 0.95$) produced only a 23% reduction in cost, still greater than the 18% from the muscle replacement strategy, but much lower than 73%. On the other hand, for a scaled muscle-force-squared cost, the ankle contribution was about 43% for a non-amputee walk and the reduction from the robotic prosthesis was about 74% (Figure S3 and Table S5, Supplementary Information). Thus, it appears that some of these specific numerical predictions may rely on the metabolic cost model and may be improved with a much more accurate metabolic cost model, which remains an open problem^{11,18}.

Having performed over a hundred different optimization calculations under different parameter conditions (in contrast to other optimization-based studies^{16–18}), we have demonstrated feasibility of using such large-scale optimizations in a formal design procedure with user-specific model parameters. Future work could consider the effects of different prosthesis structures (including non-ideal actuators and passive elements) and constraining the prosthesis torque to be a function of system state rather than be allowed to vary arbitrarily in time: for instance, by using existing controller structures found in other prostheses or by parameterizing a torque versus ankle angle relation for a gait and optimizing the controller parameters. Such additions will allow us to compare the results of our simulation to those found through experiment, and improve the model to make accurate quantitative predictions.

References

1. Lehmann, J. *et al.* Comprehensive analysis of energy storing prosthetic feet: Flex foot and seattle foot versus standard sach foot. *Arch. Phys. Med. Rehabil.* **74**, 1225–1231 (1993).
2. Burger, H., Marincek, C. & Isakov, E. Mobility of persons after traumatic lower limb amputation. *Disabil. Rehabil.* **19**, 272–277 (1997).
3. Davies, B. & Datta, D. Mobility outcome following unilateral lower limb amputation. *Prosthet. Orthot. Int.* **27**, 186–190 (2003).
4. Ganguli, S., Datta, S., Chatterjee, B. & Roy, B. Metabolic cost of walking at different speeds with patellar tendon-bearing prosthesis. *J. Appl. Physiol.* **36**, 440–443 (1974).
5. Waters, R., Perry, J., Antonelli, D. & Hislop, H. Energy cost of walking of amputees: the influence of level of amputation. *J. Bone Joint Surg. Am.* **58**, 42–46 (1976).
6. Au, S., Weber, J. & Herr, H. Powered ankle-foot prosthesis improves walking metabolic economy. *IEEE Trans. Robot.* **25**, 51–66 (2009).
7. Caputo, J. & Collins, S. Prosthetic ankle push-off work reduces metabolic rate but not collision work in non-amputee walking. *Sci. Rep.* **4**, 51–66, doi: 10.1038/srep07213 (2014).
8. Zmitrewicz, R., Neptune, R. & Sasaki, K. Mechanical energetic contributions from individual muscles and elastic prosthetic feet during symmetric unilateral transtibial amputee walking: a theoretical study. *J. Biomech.* **40**, 1824–1831 (2007).
9. LaPre, A., Umberger, B. & Sup, F. Simulation of a powered ankle prosthesis with dynamic joint alignment. In *Conf. Proc. IEEE Eng. Med. Biol. Soc.* 1618–1621 (2014).
10. Mattes, S., Martin, P. E. & Royer, T. Walking symmetry and energy cost in persons with unilateral transtibial amputations: matching prosthetic and intact limb inertial properties. *Arch. Phys. Med. Rehabil.* **81**, 561–568 (2000).

11. Srinivasan, M. Fifteen observations on the structure of energy minimizing gaits in many simple biped models. *J. R. Soc. Interface* **8**, 74–98 (2011).
12. Alexander, R. Optimization and gaits in the locomotion of vertebrates. *Physiol. Rev.* **69**, 1199–1227 (1989).
13. Ralston, H. Energy-speed relation and optimal speed during level walking. *Int. Z. Angew. Physiol.* **17**, 277–283 (1958).
14. Handford, M. & Srinivasan, M. Sideways walking: preferred is slow, slow is optimal, and optimal is expensive. *Biol. Lett.* **10**, 20131006 (2014).
15. Gerritsen, K., van den Bogert, A., Hulliger, M. & Zernicke, R. Intrinsic muscle properties facilitate locomotor control - a computer simulation study. *Motor Control* **2**, 206–220 (1998).
16. Ackermann, M. & van den Bogert, A. J. Optimality principles for model-based prediction of human gait. *J. Biomech.* **43**, 1055–1060 (2010).
17. Anderson, F. C. & Pandy, M. G. Dynamic optimization of human walking. *J. Biomech. Eng.* **123**, 381–390 (2001).
18. Miller, R. H. A comparison of muscle energy models for simulating human walking in three dimensions. *J. Biomech.* **47**, 1373–1381 (2014).
19. Minetti, A. & Alexander, R. A theory of metabolic costs for bipedal gaits. *J. Theor. Biol.* **186**, 467–476 (1997).
20. Bhounsule, P. A. *et al.* Low-bandwidth reflex-based control for lower power walking: 65 km on a single battery charge. *Int. J. Robot. Res.* **33**, 1305–1321 (2014).
21. Rebula, J. R. & Kuo, A. D. The cost of leg forces in bipedal locomotion: A simple optimization study. *PLOS ONE* **10**, e0117384, doi: 10.1371/journal.pone.0117384 (2015).
22. Martin, A. E. & Schmiedeler, J. P. Predicting human walking gaits with a simple planar model. *J. Biomech.* **47**, 1416–1421 (2014).
23. Srinivasan, M. & Ruina, A. Computer optimization of a minimal biped model discovers walking and running. *Nature* **439**, 72–75 (2006).
24. Umberger, B. R. Stance and swing phase costs in human walking. *J. Roy. Soc. Interface* **7**, 1329–1340 (2010).
25. Marler, R. & Arora, J. Survey of multi-objective optimization methods for engineering. *Struct. Multidiscip. O.* **26**, 369–395 (2004).
26. Nolan, L. *et al.* Adjustments in gait symmetry with walking speed in trans-femoral and trans-tibial amputees. *Gait Posture* **17**, 142–151 (2003).
27. Herr, H. & Grabowski, A. Bionic ankle-foot prosthesis normalizes walking gait for persons with leg amputation. *Proc. R. Soc. B.* **279**, 457–464 (2012).
28. Caputo, J. & Collins, S. A universal ankle-foot prosthesis emulator for human locomotion experiments. *J. Biomech. Eng.* **136**, 035002 (2014).
29. Sawicki, G. S. & Ferris, D. P. Powered ankle exoskeletons reveal the metabolic cost of plantar flexor mechanical work during walking with longer steps at constant step frequency. *J. Exp. Biol.* **212**, 21–31 (2009).

Acknowledgements

This work was supported by the NSF CMMI grant 1300655. Thanks to Joshua Caputo and Steven Collins (CMU) for extensive conversations informing this work.

Author Contributions

M.L.H. created the human-prosthesis model and performed the optimizations, in discussion with M.S., M.L.H. and M.S. wrote the paper together.

Additional Information

Supplementary information accompanies this paper at <http://www.nature.com/srep>

Competing financial interests: The authors declare no competing financial interests.

How to cite this article: Handford, M. L. and Srinivasan, M. Robotic lower limb prosthesis design through simultaneous computer optimizations of human and prosthesis costs. *Sci. Rep.* **6**, 19983; doi: 10.1038/srep19983 (2016).



This work is licensed under a Creative Commons Attribution 4.0 International License. The images or other third party material in this article are included in the article's Creative Commons license, unless indicated otherwise in the credit line; if the material is not included under the Creative Commons license, users will need to obtain permission from the license holder to reproduce the material. To view a copy of this license, visit <http://creativecommons.org/licenses/by/4.0/>

1 *Supplementary Information Appendix for:*

2 **Robotic lower limb prosthesis design through simultaneous**
3 **computer optimizations of human and prosthesis costs**

4 Matthew L. Handford and Manoj Srinivasan

Mechanical and Aerospace Engineering, The Ohio State University, Columbus, USA

handford.4@osu.edu, srinivasan.88@osu.edu

5 **Note.** The tables and figures in the supplementary information are numbered S1, S2, etc., whereas those in
6 the main manuscript are numbered 1, 2, etc. This Supplementary Information Appendix provides all model
7 parameters and other technical information relevant to the optimization. In addition, there is a supplementary
8 video V1 available online, the caption/legend for which is repeated below.

9 **Supplementary Video V1.** Animations of optimized human walking with a robotic prosthesis (without and
10 with a symmetry constraint), human walking with a passive prosthesis, as well as an optimized non-amputee
11 walk. For the amputee motions, we use blue for the leg with the prosthesis and gray for the leg without the
12 prosthesis.

13 **S1 Parameters**

14 The schematic (Figure S1) shows the axis conventions for the positions of the center of masses (CoM) and
15 other key body locations.

16 The biped model parameters provided in Tables S1-S3 follow those in Gerritsen et al and van den Bogert
17 tutorial [1, 2]. (The parameters are drawn directly from the van den Bogert tutorial [2], stated to be the same
18 parameters as in Gerritsen et al [1]; Gerritsen et al [1] do not actually specify the parameter values.) The

19 Alexander-Minetti-like metabolic cost dependency on muscle activation and muscle shortening velocity are
 20 shown in Figure S2 and its caption.

21 **S2 Other objective functions**

22 We chose to check the results found using the metabolic cost function described in the Methods section of
 23 the main document and Figure S2 with two other common objective functions. The first of these objective
 24 functions is a scaled force-squared and torque-squared cost function defined by:

$$\dot{C} = \frac{1}{T_{\text{stride}}} \int_0^{T_{\text{stride}}} \left[\lambda \sum_i \frac{F_i^2}{F_{\text{iso}}^2} \cdot F_{\text{iso}} v_{\text{max}} + (1 - \lambda)(\tau/r)^2 \right] dt \quad (1)$$

25 where the sum is over all muscles, F_i is the force produced by the i^{th} muscle, τ is the prosthesis motor torque,
 26 r is a scaling constant (equal to typical muscle moment arm), T_{stride} is the total time of one stride, λ is the
 27 weighting factor, and the product $F_{\text{iso}} v_{\text{max}}$ has units of power and provides appropriate scaling of the cost
 28 for various muscles as in [3]. The second objective function is a work based cost defined by:

$$\dot{C} = (\lambda \sum_i (4W_{m,i}^+ + 0.83W_{m,i}^-) + (1 - \lambda)|W_{\text{pros}}|) / T_{\text{stride}} \quad (2)$$

29 where the sum is over all muscles, $W_{m,i}^+$ is the positive muscle work, $W_{m,i}^-$ is the negative muscle work, and
 30 W_{pros} is the prosthesis work over the stride. Using either of these objective functions produced the same
 31 qualitative results in terms of energetic trade off and kinematic changes as those found with the metabolic
 32 cost function. We compared the costs of the prosthesis with those from the non-amputee tests with each
 33 objective function. The results of this analysis can be observed in table S5. The Pareto curves from each of
 34 the three objective functions used for this research are displayed in Figure S3.

35 **S3 Cost dependence on prosthesis mass**

36 After completing tests with prosthesis mass equal to 0.5 to 1.5 times the mass of the intact foot, we found a
 37 positive correlation between mass and both human and prosthesis costs. Moreover these cost rates depend

38 linearly on mass for a given λ . Figure S4 displays the linear dependence for all λ s tested.

39 **References**

40 [1] K. G. Gerritsen, A. J. van den Bogert, M. Hulliger, and R. F. Zernicke. Intrinsic muscle properties
41 facilitate locomotor control - a computer simulation study. *Motor Control*, 2:206–220, 1998.

42 [2] A. J. van den Bogert. Gait2de – a musculoskeletal dynamics model for posture and gait. In *Conference*
43 *on Dynamic Walking, Jena*, 2011.

44 [3] A.E. Minetti and R. McN. Alexander. A theory of metabolic costs for bipedal gaits. *J. Theor. Biol.*,
45 186:467–476, 1997.

46 [4] M. Srinivasan. Fifteen observations on the structure of energy minimizing gaits in many simple biped
47 models. *Journal of the Royal Society Interface*, 8:74–98, 2011.

48 [5] Roger C Woledge, Nancy A Curtin, and Earl Homsher. Energetic aspects of muscle contraction. *Mono-*
49 *graphs of the physiological society*, 41, 1985.

50 [6] M. Srinivasan. Optimal speeds for walking and running, and walking on a moving walkway. *Chaos:*
51 *An Interdisciplinary Journal of Nonlinear Science*, 19:026112, 2009.

52 [7] M. Srinivasan and A. Ruina. Computer optimization of a minimal biped model discovers walking and
53 running. *Nature*, 439:72–75, 2006.

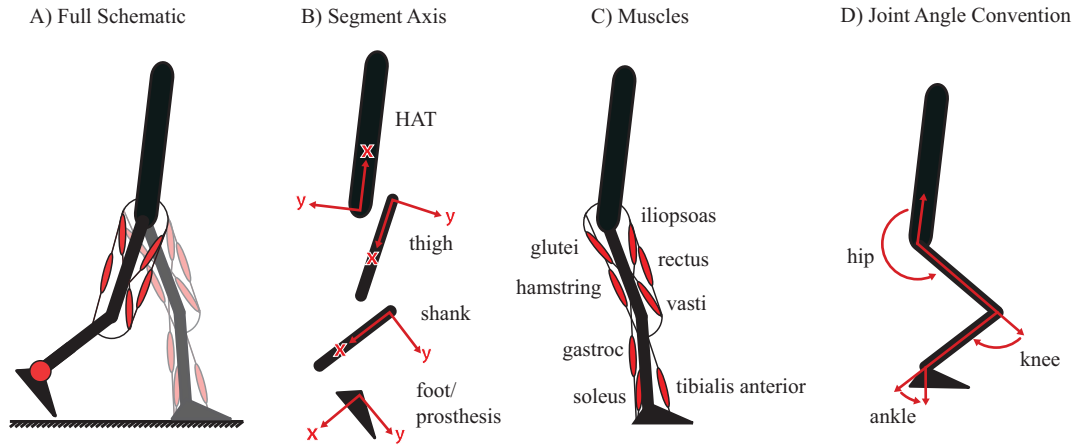


Figure S1: Biped model. A) A basic representation of the sagittal-plane human-prosthesis model. B) Origin and axis information for each of the segments. C) Graphical representation of the muscle groups. D) Joint angle convention based on rotation of relative axes with the positive direction corresponding to flexion/dorsiflexion of the joints.

Segment	Mass, kg	Moment of Inertia, kg m ²	x CoM, m	y CoM, m
HAT	50.85 (0.6879)	3.177 (47.25e-4)	0.3155 (0.3308)	0 (0)
Thigh	7.5 (0.1015)	0.1522 (22.63e-4)	0.1910 (0.2003)	0 (0)
Shank	3.49 (0.0472)	0.0624 (9.280e-4)	0.1917 (0.2010)	0 (0)
Foot	1.087 (0.0147)	0.0184 (2.736e-4)	0.0351 (0.0368)	0.0768 (0.0805)
Prosthesis	1.087 (0.0147)	0.0184 (2.736e-4)	0.0351 (0.0368)	0.0768 (0.0805)

Table S1: Biped inertia parameters. The center of mass distances are measure from the origin of the segment connected proximal joint (Figure S1b). The x distance is along the segment while y is perpendicular to the segment. Values in parentheses show the corresponding dimensionless quantity. The moment of inertia are about the z axis (perpendicular to sagittal plane), through the center of masses of the respective segments. The mass and moment of inertia for the prosthesis correspond to the standard condition where $m_{\text{pros}} = m_{\text{foot}}$

Segment	x Distance, m	y Distance, m
HAT	0.6 (0.6290)	0 (0)
Thigh	0.4410 (0.4624)	0 (0)
Shank	0.4428 (0.4642)	0 (0)
Heel (bio/pros)	0.07 (0.0734)	-0.06 (-0.0629)
Toe (bio/pros)	0.07 (0.0734)	0.15 (0.1573)

Table S2: Biped segment length and foot shape parameters. For the HAT, thigh and shank segments, the segment lengths are measured along the x axis from the origin of the segment, which is at the proximal joint (Figure S1b), to the distal joint; for these three segments, the y distance between the joints is zero, as seen in the first three rows of the table. For the foot, we show the vector from the ankle to the heel and the toe. Values in parentheses show the corresponding dimensionless quantity.

Muscle	F_{iso} , N	v_{max} , m/s	k_{tendon} , N/mm	d_{hip} , mm	d_{knee} , mm	d_{ankle} , mm
iliopsoas	1500 (2.068)	1.069 (0.3334)	264.1 (347.4)	50 (52.42)	0 (0)	0 (0)
glutei	3000 (4.137)	2.097 (0.6538)	477.7 (628.4)	-62 (-65.00)	0 (0)	0 (0)
hamstrings	3000 (4.137)	1.090 (0.3400)	224.6 (295.4)	-72 (-75.48)	-34 (-35.64)	0 (0)
rectus	1200 (1.655)	0.8492 (0.2648)	75.37 (99.15)	34 (35.64)	50 (52.42)	0 (0)
vasti	7000 (9.653)	0.9750 (0.3040)	784.8 (1032)	0 (0)	42 (44.03)	0 (0)
gastroc	3000 (4.137)	0.5766 (0.1798)	178.6 (234.9)	0 (0)	-20 (-20.97)	-53 (-55.57)
soleus	4000 (5.516)	0.5766 (0.1798)	408.2 (536.9)	0 (0)	0 (0)	-53 (-55.57)
tibialis anterior	2500 (3.448)	0.8597 (0.2681)	197.2 (259.3)	0 (0)	0 (0)	37 (38.79)

Table S3: Biped muscle parameters. A table displaying the max isometric force F_{iso} , max contractile velocity v_{max} , tendon stiffness k_{tendon} , and moment arm d at each joint for all 8 muscle groups. The moment arms marked as zero indicate that the muscle does not cross that joint. These muscle groups are shown graphically in Figure S1c. We ignore the muscles' force-length dependence conventional in Hill-type muscle models. The prosthesis torque is bounded by 175 Nm (0.253 non-dimensional). All parameters from [1, 2]. We use a linear force velocity relation, defined by the two parameters F_{iso} and v_{max} .

Joint	Angle lower bound	Angle upper bound
Hip	1.571	6.2831
Knee	0.05	1.885
Ankle	-0.9599	0.3491
Prosthesis	-0.9599	0.3491

Table S4: Biped joint ranges of motion. The joint angles are displayed graphically in Figure S1d. This table presents the bounds on these angles (in radians). Some bounds are assumed to be larger than anatomical, but such bounds are never active at the optimal solution, as is clear from the optimal kinematics depicted in the main manuscript (Figure 2).

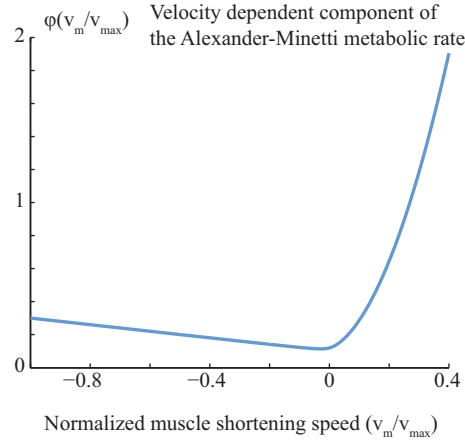


Figure S2: Metabolic cost details. The metabolic cost expression adapted from [3, 4], has two terms: an activation cost ψ and a muscle-shortening related term ϕ . The muscle-shortening related term ϕ , depicted in this figure, is based on empirical heat and ATPase activity [3] and approximated by $\phi = 0.1 + 0.9(\bar{v})^+ + 0.2(\bar{v})^- + 9(\bar{v})^+(\bar{v})^+$, where \bar{v} is the muscle contractile velocity over the maximum contractile velocity, $(\bar{v})^+$ is the positive part of the \bar{v} , and $(\bar{v})^-$ is the negative part of \bar{v} . This function is used to model the differing metabolic cost between a contracting muscle and an extending muscle. See [4] for more details. The activation cost $\psi(a_i) = 0.05(a_i + a_i^2)$ is a function that captures the empirical result that about 40% of isometric muscle exertion cost is the activation cost [5]. Because we optimize for a fixed walking speed, we do not include a resting cost to the total metabolic cost. Adding a fixed resting metabolic rate will simply add a constant term to all the metabolic costs and does not change any of the optimal strategies [6].

Objective function	Non-amputee	Replacement strategy (% reduction)	Amputee (% reduction)
Alexander-Minetti	0.1054	0.0622 (41%)	0.0312 (73%)
Force-squared	0.0547	0.0319 (42%)	0.0143 (74%)
Work-based	0.0437	0.0357 (18%)	0.0335 (23%)

Table S5: Other objective functions. The non-dimensional human cost using Alexander-Minetti, Force-squared, and work-based costs.

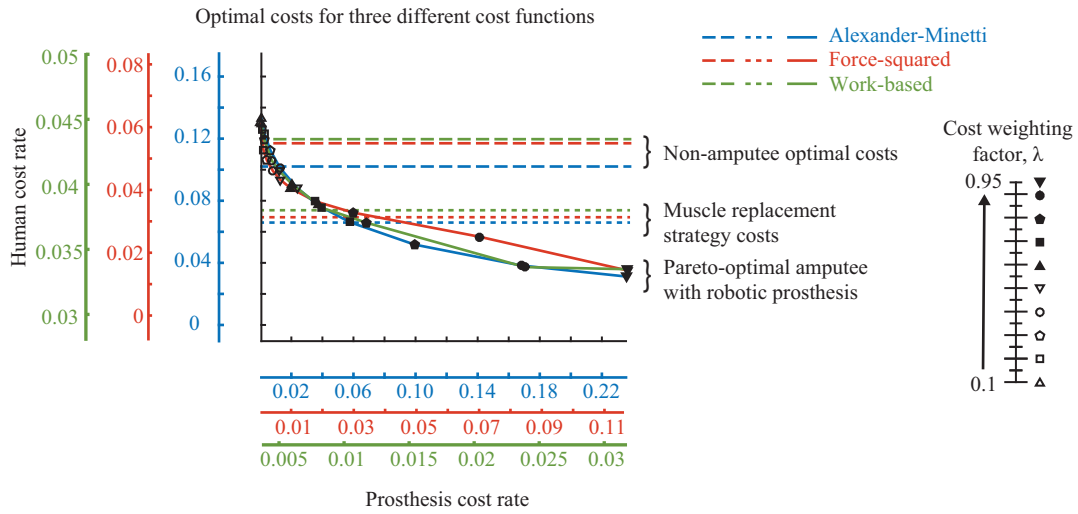


Figure S3: Pareto curves for two other cost models. Pareto curves for three different cost functions are shown (solid curves): (1) using Alexander-Minetti cost for human and smoothed torque-squared cost for prosthesis, as in the main manuscript (Figure 3A), (2) using a scaled muscle-force-squared cost for the human and a scaled torque-squared cost for the prosthesis, (3) using a muscle work-based cost for the human and a motor work cost for the prosthesis. Thus, these Pareto curves show that all these different costs give qualitatively similar trade-offs between human and prosthesis energy costs for the amputee. The work based costs produced impulsive muscle forces and prosthesis torques, as also observed in earlier work [4, 7]. For the three cost functions, we also show the optimal costs for an able-bodied (non-amputee) walker (long-dashed line) and that for the “muscle replacement strategy” (short-dashed line), demonstrating that the optimal robotic prosthesis actuation reduces amputee energy cost below both the able-bodied walker and an able-bodied walker with cost-free muscles crossing an ankle.

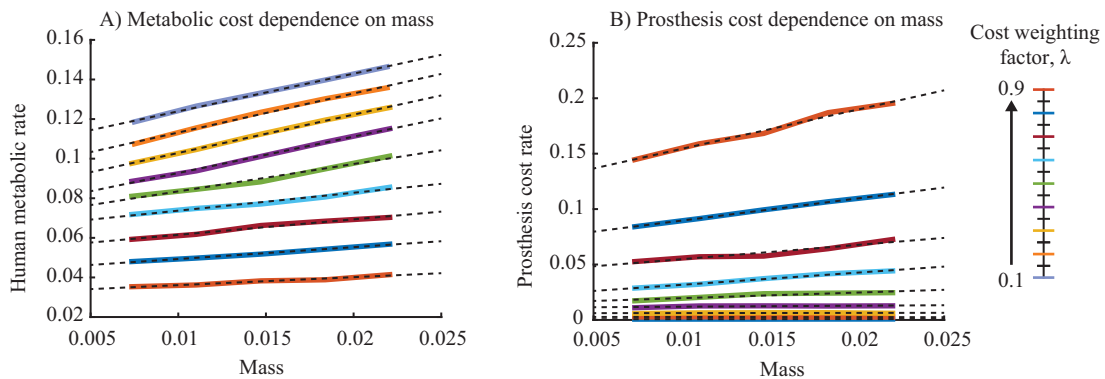


Figure S4: Linear dependence of cost on prosthetic foot mass. Linear-dependence on mass of (A) human metabolic cost rate and (B) prosthesis cost rate.

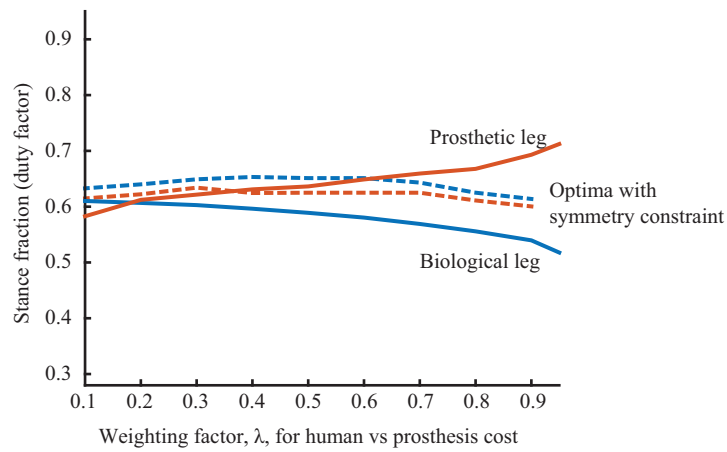


Figure S5: Duty factor. Duty factor (a leg’s stance duration as a fraction of total stride period) is shown for the two legs for the Pareto-optimal amputee walking, as a function of the weighting factor λ . When asymmetric gaits are allowed (solid lines), we find that the prosthetic leg spends more time in stance than the biological foot as λ is increased, presumably to allow the prosthesis to provide more assistance. When we have symmetry constraints (dashed lines), we find that the two legs have slightly different stance periods because the symmetry constraint does not impose perfect symmetry.